A catalyst-free and green method for synthesis of 9-substituted-9H-diuracilopyrans in magnetized water: experimental aspects and molecular dynamics simulation

Mohammad Bakherad[1] · Zainab Moosavi-Tekyeh[1] · Ali Keivanloo[1] · Mostafa Gholizadeh[2] · Zahra Toozandejani[1]

Abstract The reactions of aldehydes and barbituric acid at low temperatures in magnetized water, as a green-promoting medium, provides 9-substituted-9H-diuracilopyrans in high-to-excellent yields. This method offers the advantages of short reaction times, simplicity, low costs, high reaction yields, being green, and no need for any organic solvent. Moreover, the influence of magnetized water on the reactivity of the reactants is investigated using molecular dynamics simulations. It is shown that magnetized water has a dramatic impact on the reactivity of the two reactants involved through increase in the strength of the hydrogen bond interactions between them.

Keywords Catalyst-free · Diuracilopyran · Magnetized water · Molecular dynamics simulation · Hydrogen bond interaction

Introduction

Pyrimidine-triones are one of the most broadly distributed groups of natural compounds. Most pyrimidine-trione derivatives have several biological properties such as the anti-tumor, anti-cancer, HIV-1 and HIV-2 protease inhibitors, anti-convulsant, and anti-osteoporosis activities [1–4]. Moreover, 4H-pyrans play a vital role in the manufacture of various biologically active drugs with anti-convulsant [5],

✉ Mohammad Bakherad
  m.bakherad@yahoo.com

  Zainab Moosavi-Tekyeh
  ztmoosavi@gmail.com

[1] School of Chemistry, Shahrood University of Technology, Shahrood 3619995161, Iran

[2] Department of Chemistry, Ferdowsi University of Mashhad, Mashhad 91779, Iran

 Springer

anti-microbial [6], anti-coagulant, spasmolytic, anti-cancer, and anti-anaphylactic activities [7]. On the other hand, a more pronounced effect is generally observed when two or more different heterocyclic moieties exist in a single molecule, because it might possess the properties of all moieties and enhance the pharmacological activities. In this regard, we sought to explore a single structural framework by combining the 4H-pyran and barbituric acid motifs that could show promising medical properties. Nevertheless, only a few reports are related to the preparation of diuracilopyrans. One of the typical methods used for the synthesis of diuracilopyran derivatives involves the condensation of aldehydes with pyrimidine-trione (barbituric acid) in the presence of a catalyst [8–10]. However, many of these synthetic methods face a number of disadvantages like using toxic solvents and reagents/catalysts, and having tedious steps, low product yields, and long reaction times, which limit their use in practical applications. In order to overcome these problems, the development of a catalyst-free, milder, cheaper, more general, and highly-efficient as well as an environmentally benign method, is desirable for constructing diuracilopyrans. Solvents define a chief part of the environmental performance of processes in the chemical industry, and also have an effect on the safety, cost, and health issues. The notion of green solvents points out the goal to minimize the environmental effects resulting from the use of solvents in chemical production. Due to its exclusive structure and physico-chemical properties, water leads to specific interactions like hydrogen bonding and the hydrophobic effect. It is also regarded as an environmentally benign and a green solvent, and thus a very large number of efforts have been made to develop catalytic processes using water as a medium to acquire a greener synthesis [11]. Besides, reactions in water lead to an enhanced product yield, a shorter reaction time, and a greater ease of manipulation.

The design and exploration of novel catalyst-free methods for pharmacological agents in aqueous media is an ideal option and a major challenge for chemists to reduce the ecological problems and economic burden [12]. In this context, multi-component reactions that can take place in water have been considerably followed in the past few years because of their effective atom economy and green characteristics [13]. These reactions are efficient in preparing highly-functionalized small organic molecules from readily available starting materials in one step with inherent flexibility for producing molecular diversity and complexity coupled with minimization of cost, time, labor, and waste production [14]. Moreover, these reactions frequently yield excellent regio- and chemo-selectivities [15].

We have known that water can be magnetized in the presence of an external magnetic field, although the effect is minute [16–18]. Based upon the literature surveys done on magnetized water during the recent years, most researchers have been interested in studying the magnetic field effects on the properties of water, especially the hydrogen bond distribution [19].

Furthermore, many researchers have studied the effect of magnetized water on the morphology of the precipitated calcium carbonate [20], synthesis of manganese oxide nano-crystals [21], and TiO$_2$-based varistors [22]. Very recently, we have described the synthesis of pyranopyrazole derivatives using magnetized water as a solvent [23]. Here, we wish to report the catalyst-free synthesis of 9-substituted-9H-

diuracilopyrans **3** via one-pot three-component reactions of barbituric acid **1** with various aldehydes **2** in magnetized water (Scheme 1).

Furthermore, the effect of magnetized water in the synthesis of diuracilopyrans was investigated by theoretical studies. Molecular dynamics (MD) simulation is a modern tool and powerful complementary approach to an experiment at the atomic level. An MD simulation can explore and elucidate the microscopic details on the interactions between reactants, and further, explain the experimental results to gain insight into the physical mechanisms behind interactions in various systems [24, 25]. Although in some recent research works, the effect of an external magnetic field on the structure of reactants by MD simulations has been investigated [26, 27], the influence of magnetized water on the reactions has not yet been reported. In this work, MD simulation contributes to the overall effort to understand the effect of a magnetized water on the structural behavior of reactants. With the aid of MD simulation, the reactants [i.e., benzaldehyde (BA) and barbituric acid (BaAc)] were equilibrated in two different media (non-magnetized and magnetized water), and then the structural properties (including hydrogen-bond interaction of water with reactants) were investigated by radial distribution functions. The so-called pure (non-magnetized) water having a pH value of about 7.1 consists of deionized water molecules, and magnetized water is pure water that has been exposed to an external magnetic field (0.6 T).

Experimental

The reagents and solvents used were supplied from Merck, Fluka or Aldrich. Melting points were determined using an electro-thermal C14500 apparatus. The reaction progress and the purity of compounds were monitored using TLC analytical silica gel plates (Merck 60 F250). All the known compounds were identified by comparing their melting points and ^{1}H NMR data with those in the authentic samples. The ^{1}H NMR (300 MHz) and ^{13}C NMR (75 MHz) spectroscopies were run on a Bruker Advance DPX-250 FT-NMR spectrometer. The chemical shift values were given as δ values against tetramethylsilane (TMS) as the internal standard, and the J values were given in Hz. Micro-analysis was performed on a Perkin-Elmer 240-B micro-analyzer.
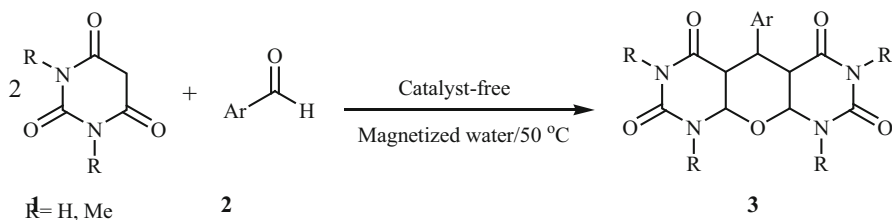
Scheme 1 Catalyst-free synthesis of diuracilopyrans in magnetized water

Preparation of magnetized water

Magnetized water was prepared according to our earlier report [23]. A magnetic treatment apparatus was assembled as shown in Fig. 1. This apparatus was equipped with a powerful magnet (0.6 T). A centrifugal pump was used to circulate water in the system. Water was treated in the system for 5 min, and 100 mL of the resulting magnetized water was then used in the current work.

General procedure for synthesis of 9-substituted-9*H*-diuracilopyran (3a-o)

To a 10-mL round-bottomed flask equipped with a magnetic stirrer bar and containing magnetized water (5 mL, with a magnetization time of 5 min), were added an aldehyde (1.0 mmol) and barbituric acid or *N,N*-dimethylbarbituric acid (2.0 mmol). The reaction mixture was stirred at 50 °C, and the reaction progress was monitored by TLC using chloroform as the eluent. After completion of the reaction, the precipitate formed was filtered and purified by recrystallization from ethanol to afford the desired product (Table 2).
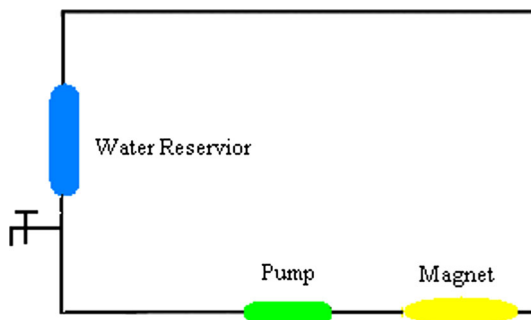
9-(4-Methylphenyl)-9H-diuracilopyran (3b)

IR (KBr): 3232, 3095, 2900, 1744, 1680, 1640, 1550 cm^{-1}; ^{1}H NMR (300 MHz, DMSO-d_6) δ 2.39 (s, 3H, CH$_3$), 4.19 (s, 1H, CH), 6.68 (s, 2H, NH); 7.29 (d, 2H, *J* 8.1 Hz, Ar–H), 8.09 (d, 2H, *J* 8.1 Hz, Ar–H), 11.23 (s, 1H, NH); 11.38 (s, 1H, NH); ^{13}C NMR (75 MHz, DMSO-d_6) δ 21.8, 37.4, 79.8, 129.3, 134.4, 143.9, 150.6, 162.2, 164.0; Anal. Calcd for C$_{16}$H$_{12}$N$_4$O$_5$: C, 56.47; H, 3.55; N, 16.46; found: C, 56.30; H, 3.45; N, 16.63.

9-(4-Fluorophenyl)-9H-diuracilopyran (3f)

IR (KBr): 3232, 3088, 2864, 1712, 1699, 1683, 1446 cm^{-1}; ^{1}H NMR (300 MHz, DMSO-d_6) δ 4.25 (s, 1H, CH), 7.25–7.33 (m, 2H, Ar–H), 7.52–7.60 (m, 1H, Ar–H), 7.93–7.98 (m, 1H, Ar–H), 8.28 (s, 2H, NH); 11.30 (s, 1H, NH); 11.48 (s, 1H, NH); ^{13}C NMR (75 MHz, DMSO-d_6) δ 38.1, 79.1, 115.5, 115.8, 133.9, 134.0, 142.0,

Fig. 1 Pilot of magnetic apparatus

151.0, 151.1, 159.3, 161.5, 162.6, 163.1; Anal. Calcd for $C_{15}H_9FN_4O_5$: C, 52.33; H, 2.64; N, 16.27; found: C, 52.48; H, 2.75; N, 16.44.

9-(3-Fluorophenyl)-9H-diuracilopyran (3g)

IR (KBr): 3216, 3097, 2960, 1750, 1670, 1568, 1440 cm^{-1}; ^{1}H NMR (300 MHz, DMSO-d_6) δ 4.11 (s, 1H, CH), 7.35–7.39 (m, 1H, Ar–H), 7.48–7.55 (m, 1H, Ar–H), 7.76 (d, 1H, J 7.8 Hz, Ar–H), 8.0–8.04 (m, 1H, Ar–H), 8.26 (s, 2H, NH); 11.31 (s, 1H, NH); 11.46 (s, 1H, NH); ^{13}C NMR (75 MHz, DMSO-d_6) δ 36.5, 81.1, 113.1, 117.0, 122.9, 130.3, 142.0, 152.6, 153.0, 160.1, 161.9, 163.3, 163.5; Anal. Calcd for $C_{15}H_9FN_4O_5$: C, 52.33; H, 2.64; N, 16.27; found: C, 52.50; H, 2.73; N, 16.10.

9-(4-Bromophenyl)-9H-2,4,5,7-tetramethyl-diuracilopyran (3k)

IR (KBr): 3302, 3104, 2936, 1728, 1667, 1587, 1568 cm^{-1}; ^{1}H NMR (300 MHz, DMSO-d_6) δ 3.18 (s, 6H, N-CH$_3$), 3.24 (s, 6H, NCH$_3$), 4.60 (s, 1H, CH), 7.67 (d, 2H, J 8.7 Hz, Ar–H), 7.93 (d, 2H, J 8.7 Hz, Ar–H); ^{13}C NMR (75 MHz, DMSO-d_6) δ 28.5, 29.0, 36.1, 80.1, 120.0, 131.5, 131.7, 132.7, 142.8, 153.6, 154.3, 160.7, 162.4; Anal. Calcd for $C_{19}H_{17}BrN_4O_5$: C, 49.47; H, 3.71; N, 12.15; found: C, 49.62; H, 3.80; N, 12.30.

9-(4-Chlorophenyl)-9H-2,4,5,7-tetramethyl-diuracilopyran (3m)

IR (KBr): 3415, 2928, 1760, 1712, 1696, 1664, 1625 cm^{-1}; ^{1}H NMR (300 MHz, DMSO-d_6) δ 3.16 (s, 3H, N-CH$_3$), 3.19 (s, 3H, NCH$_3$), 3.23 (s, 3H, NCH$_3$), 3.29 (s, 3H, NCH$_3$), 4.35 (s, 1H, CH), 7.59 (d, 2H, J 8.4 Hz, Ar–H), 8.08 (d, 2H, J 8.4 Hz, Ar–H); ^{13}C NMR (75 MHz, DMSO-d_6) δ 28.5, 29.0, 47.5, 79.1, 128.5, 128.1, 132.1, 137.1, 151.2, 151.5, 160.7, 162.4; Anal. Calcd for $C_{19}H_{17}ClN_4O_5$: C, 54.75; H, 4.11; N, 13.44; found: C, 54.58; H, 4.01; N, 13.62.

9-(4-Nitrophenyl)-9H-2,4,5,7-tetramethyl-diuracilopyran (3o)

IR (KBr): 3446, 3099, 2976, 1765, 1660, 1550, 1490 cm^{-1}; ^{1}H NMR (300 MHz, DMSO-d_6) δ 3.11 (s, 6H, N-CH$_3$), 3.16 (s, 6H, NCH$_3$), 4.60 (s, 1H, CH), 7.31 (d, 2H, J 8.4 Hz, Ar–H), 8.27 (d, 2H, J 8.4 Hz, Ar–H); ^{13}C NMR (75 MHz, DMSO-d_6) δ 28.5, 29.0, 43.8, 82.7, 123.3, 128.4, 140.7, 148.4, 151.7, 160.4, 166.4; Anal. Calcd for $C_{19}H_{17}N_5O_7$: C, 53.40; H, 4.01; N, 16.39; found: C, 53.23; H, 4.11; N, 16.55.

Molecular simulations

MD simulations were carried out with the optimized molecular geometry using the Gaussian 09 [28] program at the B3LYP/6-311++G* level of theory for the abovementioned reactants. The partial atomic charges were calculated using the ChelpG method at the same level of theory. In the ChelpG method, the atomic charges were derived from a least-squares fit to the electrostatic field in a large number of points around the molecule of interest [29, 30]. As the main purpose of

MD simulations in this study is to show the influence of magnetized water on the behaviour of reactants, primarily, in terms of hydrogen bond interactions, the heterogeneous external magnetic field (0.6 T) was solely applied in the z-direction to water molecules before mixing with reactants. All classical MD simulations were carried out by the DL_POLY package [31, 32].

MD simulation consists of the numerical solutions to the classical equations of motion, which for a simple system of many particles can be written as:

$$m_i \ddot{\vec{r}}_i = \vec{f}_i \quad \vec{f}_i = \frac{\partial U}{\partial \vec{r}_i}. \tag{1}$$

The forces $\vec{f}_i$ acting on the particles are usually derived from a potential energy $U(r)$. A standard form of the potential energy function used [33] is:

$$U_{\text{tot}} = \sum_{\text{bond}} k_b(r - r_0)^2 + \sum_{\text{angles}} k_\theta(\theta - \theta_0)^2 + \sum_{\text{dihedrals}} k_\chi[1 + \cos(n\chi - \delta)] \\ + \sum_{\text{improper}} k_\psi(\psi - \psi_0)^2 + \sum_{i=1}^{N-1} \sum_{j>i}^{N} \left[\varepsilon_{ij} \left(\frac{A_{ij}}{r_{ij}^{12}} - \frac{B_{ij}}{r_{ij}^{6}} \right) + \frac{q_i q_j}{r_{ij}} \right]. \tag{2}$$

The first four terms in this equation are related to the potentials of bonded interactions, and the last two terms (Lennard-Jones (12-6) and columbic potentials) represent the non-bonded interactions between the particles. Any functional form and parameter set in this equation that is used to calculate the total potential energy, U_{tot}, is known as a force field.

The optimized structure of each reactant along with OPLS all-atom force-field [34] with Lennard-Jones parameters [34, 35] as intermolecular short range dispersion describe the reactant molecules. The reactants were placed in a cubic simulation box with the cell sizes of $30 \times 30 \times 30$ Å^3, containing 1500 water molecules. The water molecules were described using the simple-point-charge (SPC) force-field [36, 37].

The long-range electrostatic interactions were handled using the Ewald procedure [38, 39] in the isothermal-isobaric (NPT) ensemble. A Nosé-Hoover barostat, and A Berendsen thermostat at 298.15 K and 1.01325 bar, and a cut-off distance of 14 Å were also applied. Positions and velocities of the particles during the equilibration process were calculated using the Verlet velocity algorithm [40] with a time step of 1 fs. After reaching the equilibrium state under ambient conditions, the obtained configurations of the mixture at NPT ensemble were applied as an input for the NVE simulation.

For pure water, the above-mentioned computational procedure was carried out, first in the absence and then in the presence of an external magnetic field. In this simulation, the external magnetic field was applied along the z-direction. The applied magnetic force field, F_B, can be formulated by the known Lorentz force equation as follows:

$$\vec{F}_{\mathrm{B}} = q\left(\vec{V} \times \vec{H}\right), \tag{3}$$

where $\vec{H}$ is the flux density of the magnetic field, and q and $\vec{V}$ are the charge and velocity of the charged particles, respectively. The algorithm used in the DL_POLY package for describing the movement of the charged particles in an external magnetic field has been presented in Ref. [41].

In the present work, initially, the MD simulation of the reactants was performed in the non-magnetized water (pure water), and then the results of radial distribution function (RDF), and hydrogen bond interactions in this situation were compared with that of a mixture of reactants in the presence of magnetized water. In the Lorenzen viewpoint [42–44], the information for the magnetic field can be stored in the electronic memory of the magnetized water molecules.

In statistical mechanics, RDF, noted as $g(r)$, in a system of particles, describes the probability of finding any particle at a distance r from the reference one. RDF is defined as follows:

$$g(r) = \frac{\rho_r}{\rho_0} = \frac{n(r)/V(r)}{n_0/V_0} \approx \frac{n(r)}{4\pi^2 \rho_0 \delta r}, \tag{4}$$

where ρ_r and ρ_0, respectively, are the atomic densities in every spherical shell and in the whole system from the reference particle that is placed in the centre of the inner spherical shell, and r and δr, respectively, are the radius and the thickness of the spherical shell, and $V(r)$ and V_0 are the volumes of the spherical shell and the whole system, respectively. In this equation, the atomic number in the spherical shell and the whole system, respectively, are denoted by $n(r)$, and n_0. Therefore, we can use RDFs to analyze the structural properties and the hydrogen bond interactions. One of the geometric criteria involved in the formation of hydrogen bonds is the position of the first minimum of the intermolecular O⋯H RDFs (around 2.5 Å) [45, 46].

Results

Magnetized water was prepared using a static magnetic system of 6000 G field strength, according to our previous report [23].

At the beginning of this work, the reaction of barbituric acid (BaAc) with benzaldehyde (BA) was chosen as a model reaction to establish the optimum reaction conditions. This reaction was performed in normal water in the absence of any catalyst to establish the real efficacy of the magnetized water. As it can be seen in Table 1, only a low product yield was obtained even after the reaction time was lengthened to 5 h at 50 °C (Table 1, entry 1). To optimize the reaction conditions, the above model reaction was carried out under different reaction conditions. After screening various magnetized water, it was noticed that the best product yield **3a** was found in water magnetized in 5 min and for a reaction time of 10 min at 50 °C (Table 1, entry 3). Increasing the reaction time (Table 1, entry 5) and reaction temperature (Table 1, entry 6) did not improve the product yield.

Table 1 Synthesis of 9-phenyl-9*H*-diuracilopyran **3a** under various conditions

Entry	Solvent	Magnetization time (min)	Temp. (°C)	Reaction time (min)	Yield (%)[a]
1	Doubly distilled water	Non-magnetized	50	300	20
2	Magnetized water	2	50	10	97
3	Magnetized water	5	50	10	97
4	Magnetized water	10	50	10	97
5	Magnetized water	5	50	120	96
6	Magnetized water	5	70	10	96

Reaction conditions: BA (1.0 mmol), BaAc (1.0 mmol), solvent (5 mL)

[a] Isolated yield

Following our work to synthesize 9-substituted-9*H*-diuracilopyran **3** via a three-component reaction, the best conditions (Table 1, entry 3) were applied to various aromatic aldehydes to give the related 9-substituted-9*H*-diuracilopyrans **3** in high-to-excellent yields (Table 2). As shown in this table, aromatic aldehydes having electron-withdrawing groups reacted at faster rates compared with those having electron-releasing groups.

Interestingly, at the beginning of the reactions, a solution that seemed to be transparent was observed because aldehydes and barbituric acid were soluble in magnetized water. The latter formed a product, which was found to be insoluble in magnetized water. At the end of the reaction, a large amount of the solid product was formed.

Discussion

The optimized structure and atomic labels for BA and BaAc are shown in Fig. 2.

With RDF for some interactions between BA and BaAc in aqueous solution, we found out the structural changes for the abovementioned reactants in magnetized water. We first focused on the RDFs related to hydrogen bonding (H-bond), i.e., $g_{O\_2\cdots H\_N3}$ and $g_{O\_2\cdots H\_C3}$ (Fig. 3) because the H-bond plays a crucial role in determining the thermodynamic and kinetic properties of many reactions. As shown in Fig. 3, the O_2···H_N3 and O_2···H_C3 RDF results indicate that the maximum peaks in magnetized water are around 2.0 and 2.75 Å, respectively. These distances, which are between the oxygen atom of BA and the hydrogen atoms of amine and methylene groups in BaAc, are slightly influenced in magnetized water compared with non-magnetized water. As shown in this figure, the height of the first peak increases in magnetized water, which indicates that more BA and BaAc molecules interact with each other compared to unmagnetized water. This implies that magnetized water causes more attractive forces between the BA and BaAc

Table 2 Synthesis of 9-substituted-9H-diuracilopyrans **3**

Entry	R	Ar	Product	Reaction time(min)	Yield (%)[a]	MP (ºC)	MP (ºC) [ref.]
1	H	Ph	**3a**	20	90	297-299	300-301 [47]
2	H	4-Me-C₆H₄	**3b**	20	90	276-278	This work
3	H	4-MeO-C₆H₄	**3c**	20	85	290-293	288-292 [47]
4	H	4-Br-C₆H₄	**3d**	10	95	309-311	310-312 [48]
5	H	4-Cl-C₆H₄	**3e**	10	100	306-308	305-307 [47]
6	H	4-F-C₆H₄	**3f**	10	95	238-240	This work
7	H	3-F-C₆H₄	**3g**	10	95	295-297	This work

Table 2 continued
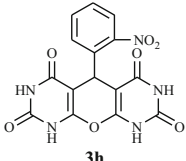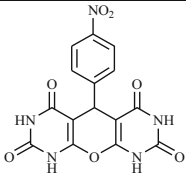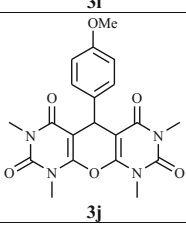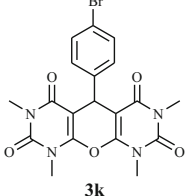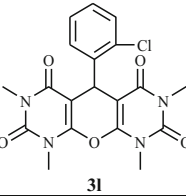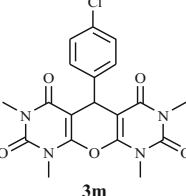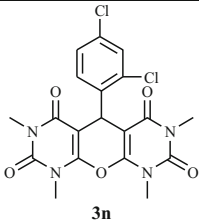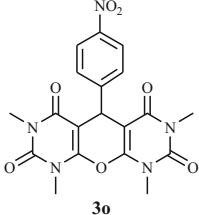
Entry	R	Ar	Product	Reaction time(min)	Yield (%)[a]	MP (ºC)	MP (ºC) [ref.]
8	H	2-NO$_2$-C$_6$H$_4$	**3h**	10	85	272-274	270-272 [48]
9	H	4-NO$_2$-C$_6$H$_4$	**3i**	10	95	267-269	268-270 [48]
10	Me	4-MeO-C$_6$H$_4$	**3j**	20	85	250-252	249-251 [47]
11	Me	4-Br-C$_6$H$_4$	**3k**	10	95	280-282	This work
12	Me	2-Cl-C$_6$H$_4$	**3l**	10	90	200-202	200-202 [47]
13	Me	4-Cl-C$_6$H$_4$	**3m**	10	100	274-276	This work

Table 2 continued

Entry	R	Ar	Product	Reaction time(min)	Yield (%)[a]	MP (ºC)	MP (ºC) [ref.]
14	Me	2,4-Cl₂-C₆H₃	**3n**	10	85	257-259	259-260 [47]
15	Me	4-NO₂-C₆H₄	**3o**	10	95	269-271	This work

Reaction conditions: Aldehyde (1.0 mmol), barbituric acid (2.0 mmol), magnetization time (5 min), magnetized water (5 mL), at 50 °C
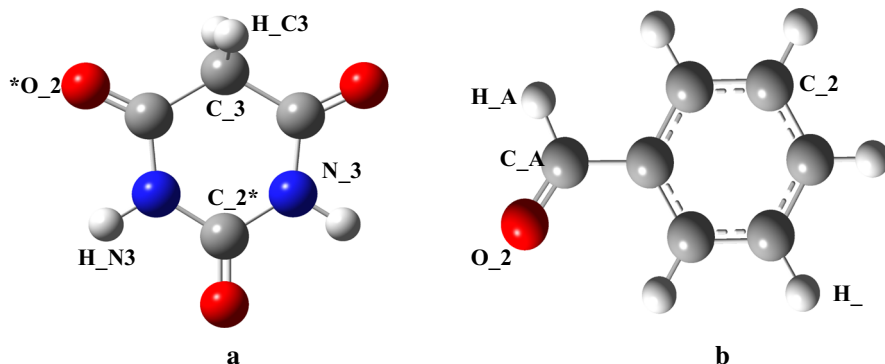
[a] Isolated yield

Fig. 2 DFT-optimized stable configurations of **a** BaAc and **b** BA with atomic labels

molecules, hence, enhancing the interactions between them, which can cause an increase in the reaction rate.

The RDFs for C_2-C_2, C_A-C_A, C_A-O_2, O_2-O_2, H_A-H_A, and H_A-O_2 for the BA–BA interactions and the RDFs for C_2-H_N3, C_2-O2*, C_2-C_2*, C_2-C_3, C_2-N3, H_A-O_2*, H_-O_2*, O_2-C_2*, and O_2-C_3 for the BA-BaAc interactions are shown in Figs. 4 and 5, respectively.

In Fig. 4, the RDF diagram of each atom pair in the BA molecules indicates that the position of the first peak in magnetized water shifts to a bigger distance compared with that in non-magnetized water, and also there is an obvious reduction
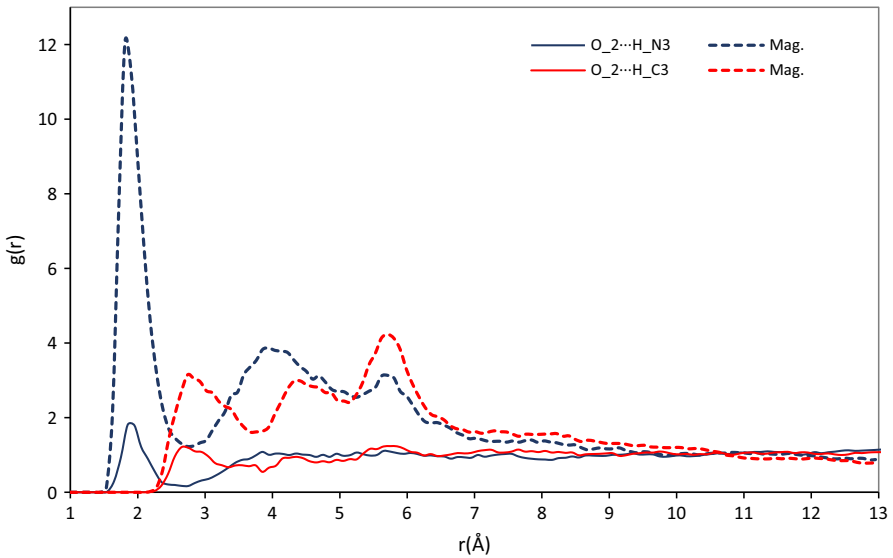
Fig. 3 Comparison of $g_{O2\cdots H\_N3}$ and $g_{O2\cdots H\_C3}$ in the pure (*solid line*) and magnetized water (*dashed line*)

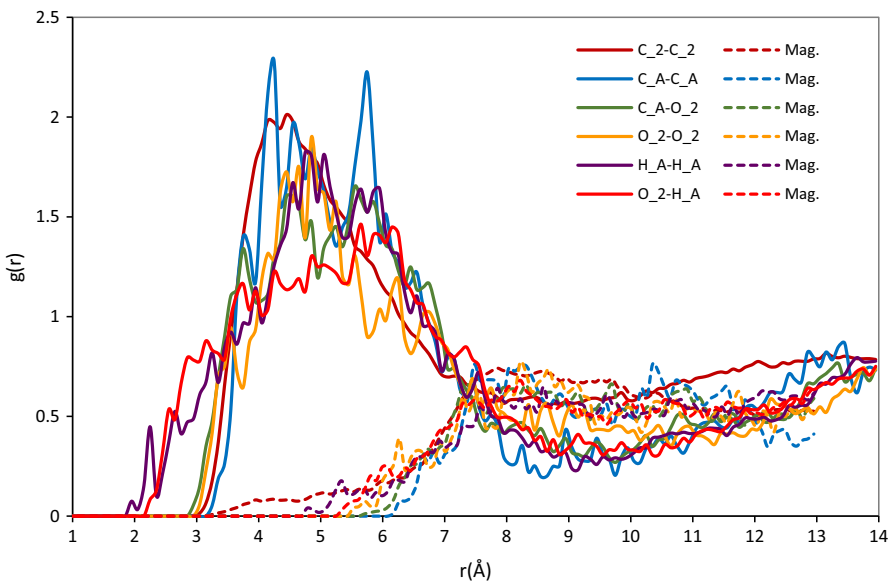**Fig. 4** Comparison of BA RDFs in the pure water (*solid line*) and magnetized water (*dashed line*)

in the height of peaks in treated water. According to these results, the BA molecules tend to be more away from each other in the magnetized water.

However, a comparison between the positions of the first peaks in each set of RDF profiles for the BA and BaAc molecules (Fig. 5) clearly indicates that the
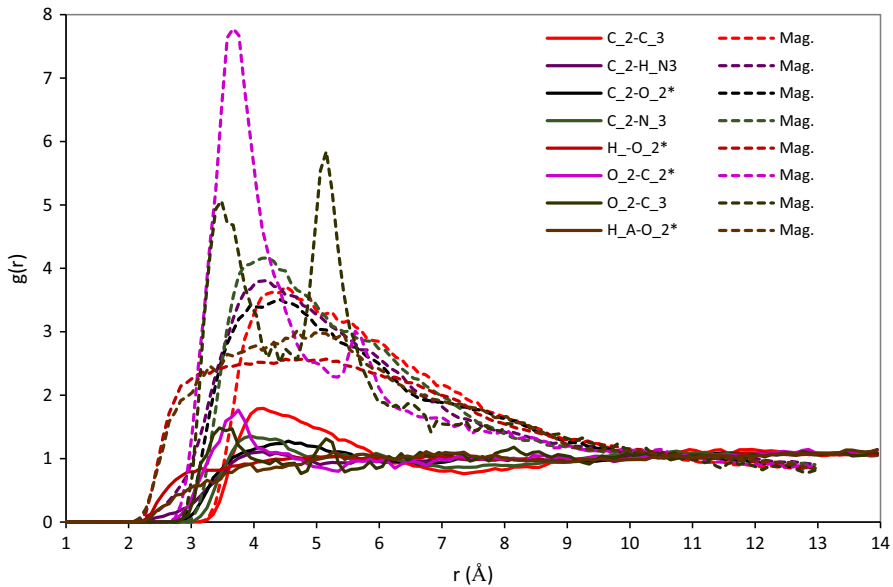
Fig. 5 Comparison of BA-BaAc RDFs in the pure water (*solid line*) and magnetized water (*dashed line*)
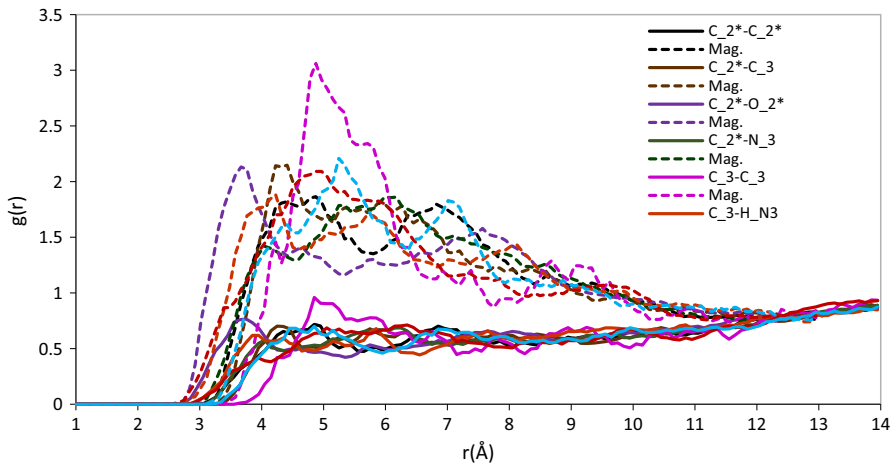

Fig. 6 Comparison of BaAc RDFs in the pure and magnetized water

distance between the BA and BaAc molecules decreases by approximately 0.5 pm, and so there are more connections between the BA and BaAc molecules in all directions, and BA molecules can be considerably more reactive in magnetized water than in non-magnetized water.

As shown in Fig. 6, RDFs of atoms in BaAc molecules suggest an obvious local existence of the BaAc molecules in the mixture. In this figure, the height of peaks increases considerably after BaAc molecules dissolve in magnetized water. The

increased peak heights indicate that more BaAc molecules exist between the water shells. The results obtained are consistent with the higher stoichiometry of the BaAc molecules in reaction. However, the position of the first peak in each set of RDF profiles is unchanged, indicating that the distance between the atoms belonging to the two next nearest neighbours and the average interaction length are not influenced by treated water, and that the solubility of BaAc molecules does not change in magnetized water.

Conclusions

We described an environmentally friendly method for the catalyst-free one-pot three-component reaction of aldehydes, and barbituric acid or *N,N*-dimethylbarbituric acid in magnetized water. This method not only offers substantial improvements in the reaction rates and yields but also avoids the use of catalysts or solvents. Also, this method offers several advantages like shorter reaction time, cleaner reaction, simple work-up procedure, being green, and high reaction yield. Furthermore, with the aid of MD, we investigated how magnetized water, as a reaction medium, can affect the rate reaction and increase the chemical reactivity at the molecular level. Although the mechanism of the effect of magnetic field is not well-understood, it is believed that a magnetized water of specific diffusion and viscosity can excite new hydrogen bondings in the reactants. These new H-bonds can be one of the most important factors of reactivity of two reactants in this reaction. The experimental evidence for more reactivity is also in agreement with this theoretical computation.

References

1. L.S. Goodman, A. Gilman, *The Pharmacological Basis of Therapeutics* (Mc Graw-Hill, New Delhi, 1991), pp. 358–360
2. G. Andrews, *Medical Pharmacology* (The CV Mosby Co., Saint Louis, 1976), pp. 243–250
3. W.O. Foye, *Principles of Medicinal Chemistry* (Lea & Febiger, Pennsylvania, 1989), pp. 143–237
4. D.J. Guerin, D. Mazeas, M.S. Musale, F.N.M. Naguib, O.N.A. Safarjalani, M.H. Kouni, R.P. Panzica, Bioorg. Med. Chem. Lett. **9**, 1477 (1999)
5. A.H. Bedair, N.A. El-Hady, M.S.A. El-Latif, A.H. Fakery, A.M. El-Agrody, Farmaco **55**, 708 (2000)
6. S.C. Kuo, L.J. Huang, H. Nakamura, J. Med. Chem. **27**, 539 (1984)
7. L. Loy, G. Bonsignore, D. Secci, A. Calignano, Eur. J. Med. Chem. **28**, 517 (1993)
8. A. Sachar, P. Gupta, S. Gupta, R.L. Sharma, Ind. J. Chem. **48B**, 1187 (2009)
9. R. Ghorbani-Vaghei, Z. Salimi, S.M. Malaekehpoor, F. Eslami, S. Noori, RSC Adv. **4**, 33582 (2014)
10. A. Sachar, R.L. Sharma, S. Kumar, D. Kaur, J. Singh, J. Heterocycl. Chem. **43**, 1177 (2006)
11. P. Ball, *H2O: A Bibliography of Water* (Phoenix Press, London, 2000)
12. Y. Gu, R. De Sousa, G. Frapper, C. Bachmann, J. Barrault, F. Jerome, Green Chem. **11**, 1968 (2009)
13. B. Jiang, C. Li, F. Shi, S.-J. Tu, P. Kaur, W. Wever, G. Li, J. Org. Chem. **75**, 2962 (2010)
14. B. Jiang, S.-J. Tu, P. Kaur, W. Wever, G. Li, J. Am. Chem. Soc. **131**, 11660 (2009)
15. D. Enders, M.R. Huettl, C. Grondal, G. Raabe, Nature **441**, 861 (2006)
16. L. Holysz, A. Szczes, E. Chibowski, J. Colloid Interface Sci. **316**, 996 (2007)

17. M. Amiri, A.A. Dadkhah, Colloid Surf. A **278**, 252 (2006)
18. H.S. Grewal, B.L. Maheshwari, Bioelectromagnetics **32**, 58 (2011)
19. K.-T. Chang, C.-I. Weng, Appl. Phys. **100**, 043917 (2006)
20. E. Chibowski, L. Hołysz, A. Szcześ, M. Chibowski, Colloid Surf. A **225**, 63 (2003)
21. T.R. Bastami, M.H. Entezari, Ultrason. Sonochem. **19**, 830 (2012)
22. J. Li, S. Luo, W. Yao, Z. Tang, Z. Zhang, M. Alim, J. Eur. Ceram. Soc. **24**, 2605 (2004)
23. M. Bakherad, A. Keivanloo, M. Gholizadeh, R. Doosti, M. Javanmardi, Res. Chem. Intermed. **43**, 1013 (2017)
24. A.R. Leach, *Molecular Modelling: Principles and Applications* (Addison Wesley, New York, 1997)
25. R. Rahman, J.T. Foster, A. Haque, J. Phys. Chem. A **117**, 5344 (2013)
26. K.-T. Chang, C.-I. Weng, J. Appl. Phys. **100**, 043917 (2006)
27. P. Xiao-Feng, D. Bo, Physica B **403**, 3571 (2008)
28. M.J. Frisch, G.W. Trucks, H.B. Schlegel, G.E. Scuseria, M.A. Robb, J.R. Cheeseman, G. Scalmani, V. Barone, G.A. Petersson, H. Nakatsuji, X. Li, M. Caricato, A. Marenich, J. Bloino, B.G. Janesko, R. Gomperts, B. Mennucci, H.P. Hratchian, J.V. Ortiz, A.F. Izmaylov, J.L. Sonnenberg, D. Williams-Young, F. Ding, F. Lipparini, F. Egidi, J. Goings, B. Peng, A. Petrone, T. Henderson, D. Ranasinghe, V.G. Zakrzewski, J. Gao, N. Rega, G. Zheng, W. Liang, M. Hada, M. Ehara, K. Toyota, R. Fukuda, J. Hasegawa, M. Ishida, T. Nakajima, Y. Honda, O. Kitao, H. Nakai, T. Vreven, K. Throssell, J.A. Montgomery Jr., J.E. Peralta, F. Ogliaro, M. Bearpark, J.J. Heyd, E. Brothers, K.N. Kudin, V.N. Staroverov, T. Keith, R. Kobayashi, J. Normand, K. Raghavachari, A. Rendell, J.C. Burant, S.S. Iyengar, J. Tomasi, M. Cossi, J.M. Millam, M. Klene, C. Adamo, R. Cammi, J.W. Ochterski, R.L. Martin, K. Morokuma, O. Farkas, J.B. Foresman, D.J. Fox, *Gaussian 09, Revision A.02* (Gaussian, Inc., Wallingford, 2016)
29. C.M. Breneman, K.B. Wiberg, J. Comput. Chem. **11**, 361 (1990)
30. L.E. Chirlian, M.M. Francl, J. Comput. Chem. **8**, 894 (1987)
31. W. Smith, T.R. Forester, J. Mol. Graph. **14**, 136 (1996)
32. T. Forester, W. Smith, *The DL_POLY_2 Reference Manual* (Daresbury Laboratory, Daresbury, 2000)
33. S.L. Mayo, B.D. Olafson, W.A. Goddard, J. Phys. Chem. **94**, 8897 (1990)
34. W.L. Jorgensen, D.S. Maxwell, J. Tirado-Rives, J. Am. Chem. Soc. **118**, 11225 (1996)
35. S. Gautam, S. Mitra, R. Mukhopadhyay, S.L. Chaplot, Phys. Rev. E **74**, 041202 (2006)
36. E. Neria, S. Fischer, M. Karplus, J. Chem. Phys. **105**, 1902 (1996)
37. H.J.C. Berendsen, J.P.M. Postma, W.F. van Gunsteren, in *Intermolecular Forces*, ed. by B. Pullman (Reidel, Dordrecht, 1973), p. 331
38. P. Ewald, Ann. Phys. **64**, 253 (1921)
39. U. Essmann, L. Perera, M.L. Berkowitz, T. Darden, H. Lee, L.G. Pedersen, J. Chem. Phys. **103**, 8577 (1995)
40. M.P. Allen, D.J. Tildesley, *Computer Simulation of Liquids*, vol. 18 (Oxford University Press, Oxford, 1989)
41. Q. Spreiter, M. Walter, J. Comput. Phys. **152**, 102 (1999)
42. L.H. Lorenzen, US Pat. 5,711,950 (1998)
43. L.H. Lorenzen, US Pat. 6,033,678 (2000)
44. J. Pan, K.N. Zhu, M. Zhou, Z.Y. Wang, Systems, Man and Cybernetics. IEEE Inter. Conf. **5**, 5034 (2003)
45. V.J. Buch, J. Chem. Phys. **96**, 3814 (1992)
46. S. Dixit, J. Crain, W.C.K. Poon, J.L. Finney, A.K. Soper, Nature **416**, 829 (2002)
47. R. Ghorbani-Vaghei, Z. Salimi, S.M. Malaekehpoor, F. Eslami, S. Noori, RSC Adv. **4**, 33582 (2014)
48. M.P. Ivin, Russ. J. Gen. Chem. **68**, 1300 (1998)